

# Heart Rate Variability Responses to Visually Induced Motion Sickness

Emmanuel Molefi, Ian McLoughlin, and Ramaswamy Palaniappan

**Abstract**—Analysis of heart rate variability (HRV) can reveal a range of useful information regarding the dynamics of the autonomic nervous system (ANS). It is considered a robust and reliable tool to understand even some subtle changes in ANS activity. Here, we study the “hidden” characteristic changes in HRV during visually induced motion sickness; using nonlinear analytical methods, supplemented by conventional time- and frequency-domain analyses. We computed HRV from electrocardiograms (ECG) of 14 healthy participants measured at baseline and during nausea. Primarily hypothesizing evident differences in measures of physiologic complexity (SampEn; sample entropy, FuzzyEn; fuzzy entropy), chaos (LLE; largest Lyapunov exponent) and Poincaré/Lorenz (CSI; cardiac sympathetic activity, CVI; cardiac vagal index) between the two states. We found that during nausea, participants showed a markedly higher degree of regularity (SampEn,  $p = 0.0275$ ; FuzzyEn,  $p = 0.0006$ ), with a less chaotic ANS response (LLE,  $p = 0.0004$ ). CSI significantly increased during nausea compared to baseline ( $p = 0.0005$ ), whereas CVI did not appear to be statistically different between the two states ( $p = 0.182$ ). Our findings suggest that motion sickness-induced ANS perturbations may be quantifiable via nonlinear HRV indices. These findings have implications for understanding the malaise of motion sickness and in turn, aid development of therapeutic interventions to relieve motion sickness symptoms.

**Clinical relevance**— The study suggests potential indices of physiologic complexity and chaos that may be useful in monitoring motion sickness during clinical studies.

## I. INTRODUCTION

Motion sickness is a syndrome that has been ailing humans since antiquity. Given intact vestibular apparatus (i.e., labyrinthine function), and sufficient intense stimulus; everyone can succumb to motion sickness [1]. This unpleasant experience arises when the brain receives incongruent sensory signals from systems regulating proprioception, balance (i.e., vestibular function), and vision [2], [3].

The onset of motion sickness is marked by a constellation of symptoms which include, for example, eyestrain, dizziness, headache, sweating, nausea and vomiting. While motion sickness symptoms might feel benign at first, their insidious onset can negatively influence cognitive and task performance [4], [5]. Physiologically, motion sickness symptom development can elicit perturbations in autonomic functional state; whereby, the neural activity of the sympathetic nervous system is increased and that of the parasympathetic nerves is reduced.

\*E.M. was supported by an EPSRC PhD studentship at the University of Kent School of Computing (EP/T518141/1).

E.M. and R.P. are with the School of Computing, University of Kent, CT2 7NZ, Canterbury, UK (corresponding author e-mail: em576@kent.ac.uk; e-mail: r.palani@kent.ac.uk).

I.M. is with the ICT Cluster, Singapore Institute of Technology, Dover Drive, 138683, Singapore (e-mail: ian.mcloughlin@singaporetech.edu.sg).

There are numerous studies that have investigated the changes in autonomic modulation induced by motion sickness, using heart rate (HR) and heart rate variability (HRV). HRV – the time-interval variations between adjacent heartbeats – is a non-invasive objective marker of the autonomic nervous system (ANS) functional state. Using a combined HRV-fMRI approach, authors in [6] found increased HR and decreased high frequency (HF) HRV power while evaluating cortical control of cardiovagal modulation of motion sickness. Low frequency (LF) HRV power has also been found to increase during motion sickness [7], together with cardiac sympathetic index (CSI) [8]. Cardiac vagal tone (CVI) and CSI indices were proposed and validated by Toichi *et al.* [9] to robustly assess short-term cardiac autonomic function, and thus explored here as part of our Poincaré/Lorenz analysis.

Although many studies have sought to understand ANS response to motion sickness, nonlinear HRV measures, specifically sample entropy (SampEn), fuzzy entropy (FuzzyEn), and the largest Lyapunov exponent (LLE), have never been evaluated in this context, to the authors knowledge. Both SampEn and FuzzyEn are measures of time series regularity; LLE gives an estimate of levels of chaos and complexity. The rationale to investigate these nonlinear metrics emanates from the long-held assertion that the HRV signal comprises nonlinear characteristics [10]. Moreover, there exists discrepancies across studies among the widely reported linear HRV measures in response to motion sickness, particularly so regarding LF/HF ratio. For example, [11] reported no change in LF/HF during malaise whereas [12] and [13] observed increase and decrease respectively.

Thus this paper is aimed at examining nonlinear HRV metrics (i.e., SampEn, FuzzyEn, LLE) as potential candidate markers of motion sickness-induced nausea. Keeping with the theme of complexity loss theory, we hypothesize primarily that there would be evident differences in these metrics between rest and during nausea. Crucially, the nonlinear metrics examined here may deepen our understanding of the underlying dynamics of autonomic function in response to motion sickness. Supplementarily, we also report time- and frequency-domain metrics that are well-studied in the literature.

## II. METHODS

### A. Participants

All experimental protocols were conducted in accordance with the Declaration of Helsinki standards for human research and were approved by the Central Research Ethics Advisory Group (ref: CREAG015-12-2021) of the University of Kent. Participants were 14 healthy volunteers (mean age ±

S.D.  $26.7 \pm 4.0$  years, 12 female) with normal or corrected-to-normal vision. All participants provided written informed consent, and received a small honorarium (£30 Amazon gift voucher) for their participation.

### B. Experimental Setup and Protocol

The protocol contained three contiguous sections (i.e., baseline, nauseogenic visual stimulus, recovery) with duration 5-min, 20-min and 5-min respectively (Fig. 1). A nauseogenic visual stimulus (visual display of stripes with  $62.5^\circ/s$  circular shift) was developed to induce motion sickness. Participants provided nausea intensity ratings via a keypad press. Presentation of the stimulus was performed using the Psychophysics Toolbox Version 3 running on MATLAB (The MathWorks, Inc., Natick, MA, USA).

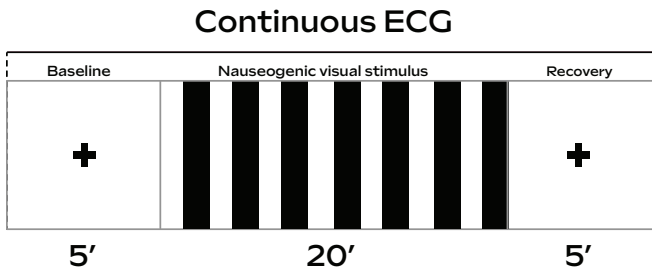


Fig. 1. Experimental overview illustration.

### C. Data Acquisition, Processing and Analysis

Electrocardiogram (ECG) signal acquisition was performed using a BioSemi ActiveTwo system (BioSemi B. V., Amsterdam, Netherlands) at a sampling rate of 256 Hz. The obtained raw ECG data was processed and analysed using custom MATLAB scripts in accordance with recommended HRV standards [14]. After a visual inspection of the ECG data for disturbances/distortions, 5-min epochs were extracted corresponding to “baseline” and “nausea” (based on nausea intensity subjective ratings) states. To generate the RR time-series, R-peak detection was first performed using the Pan-Tompkins algorithm [15]. We computed the spectra of the HRV using the Lomb-Scargle periodogram. Subsequently, we computed the total power of HRV spectra (Total Power;  $\leq 0.40$  Hz), and the power of very low frequency (VLF;  $\leq 0.04$  Hz), LF (0.04-0.15 Hz), HF (0.15-0.40 Hz) and LF/HF ratio. The LF and HF powers were computed in normalized units (n.u.), that is,  $LF_{norm} = LF / (TotalPower - VLF) * 100$  and  $HF_{norm} = HF / (TotalPower - VLF) * 100$ . We took the natural logarithm (ln) of the LF/HF ratio, that is,  $LF/HF_{ratio} = \ln(LF/HF)$ . Nonlinear Poincaré analysis was performed by computing CSI and CVI from SD1 and SD2 values using,  $CSI = SD2/SD1$  and  $CVI = \log_{10}(SD1 * SD2)$ . We further performed nonlinear dynamical analysis on the RR series via the following chaos and complexity algorithms:

1) *Sample Entropy (SampEn)*: The SampEn family of statistics is detailed in the early work of Richman and Moorman [16]. Briefly, given  $N$  points, embedding dimension  $m$  and radius of similarity  $r$ , define the correlation integral

$C_i^m(r) = \frac{N_i^m(r)}{N-m}$ , then compute average regularity with (1). The SampEn value can then be computed using (2) [16]. In this study, we use  $m = 2$  and  $r = 0.2$ , based on previous findings by others [16], [17].

$$\Phi^m(r) = \frac{\sum_{i=1}^{N-m} C_i^m(r)}{N-m}, \quad (1)$$

$$SampEn(m, r, N) = -\ln \frac{\Phi^{(m+1)}(r)}{\Phi^{(m)}(r)}. \quad (2)$$

2) *Fuzzy Entropy (FuzzyEn)*: Methodologically, FuzzyEn resembles SampEn with some exceptions; importantly, using the distance  $d_{ij}^m$  between vectors’ similarity, similarity degree is obtained by a fuzzy membership function  $\mu(d_{ij}^m, r) = e^{-\ln(2)(d_{ij}^m/r)^2}$ . From here (1) gets applied and the FuzzyEn value calculated using (3). Chen *et al.* expatiated on the FuzzyEn mechanism [18].

$$FuzzyEn(m, r, N) = -\ln \frac{\Phi^{(m+1)}(r)}{\Phi^{(m)}(r)}. \quad (3)$$

3) *Largest Lyapunov Exponent (LLE)*: The largest Lyapunov exponent ( $\lambda_1$ ) is a quantitative measure enabling characterization of chaos in HRV signals. Elaborate details of calculating  $\lambda_1$  have been presented by Rosenstein *et al.* [19]. Briefly, defining  $\lambda_1$  as  $d(t) = Ce^{\lambda_1 t}$  where  $d(t)$  is the average divergence of trajectories at time  $t$ , and constant  $C$  normalizes their initial separation; [19] shows that  $\lambda_1$  can thus be computed precisely using a least-squares fit to the “average” line defined by

$$y(i) = \frac{1}{\Delta t} \langle \ln d_j(i) \rangle, \quad (4)$$

where  $\langle \rangle$  indicates averaging over all values of  $j$ . Because of the time component in (4), we perform cubic spline interpolation at 4 Hz prior to computing the LLE value.

### D. Statistical Analysis

All statistical analyses were performed using MATLAB. Data are reported as mean  $\pm$  standard error of the mean (SEM). We compared HRV variables between baseline and nausea states using paired  $t$ -tests. Further, we computed Pearson’s correlation coefficient among autonomic variables that reached statistical significance from the  $t$ -tests. All statistical tests were two-tailed at ( $p < 0.05$ ).

## III. RESULTS

We observed that during motion sickness-induced nausea, participants exhibited a high degree of regularity; that is, lower values of SampEn and FuzzyEn, compared to baseline (Table I). All values of the LLE were positive; a feature of physiologic chaos. Contrasting LLE responses at baseline with those during nausea state showed significantly reduced chaos activity in the physiology of the participants (Table I).

Fig. 2 shows Poincaré plots from two example participants during baseline and nausea states. The shapes of the Poincaré plots reveal to us alterations of sympathetic and parasympathetic modulation [20] between baseline and nausea. We can

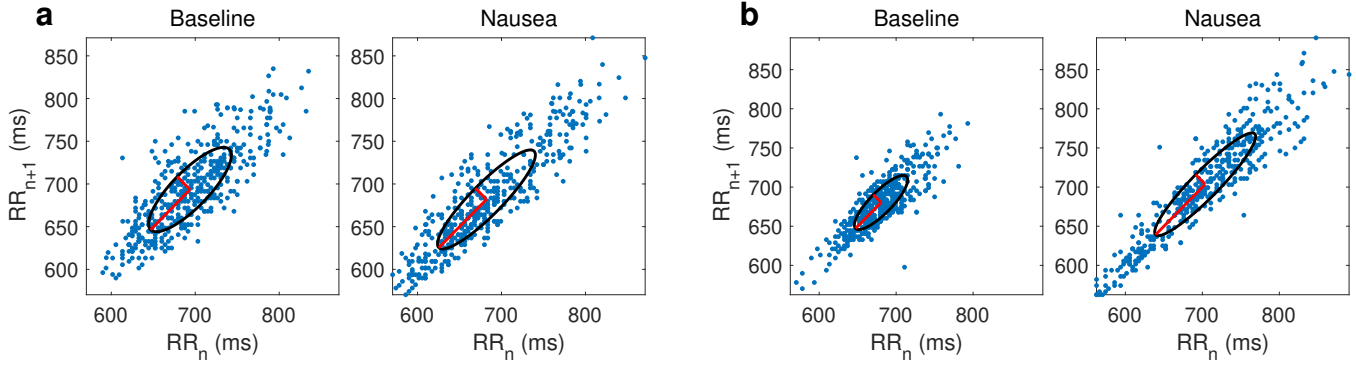


Fig. 2. Poincaré plots illustrations for Baseline and Nausea states for two example participants.

TABLE I

A SUMMARY OF THE RESULTS. DATA ARE MEAN  $\pm$  SEM.

Autonomic parameters	Baseline	Nausea	<i>p</i> -value
HR (bpm)	70.06 $\pm$ 2.91	72.57 $\pm$ 2.73	0.0258
SDNN (ms)	62.07 $\pm$ 6.94	73.14 $\pm$ 8.09	0.0136
RMSSD (ms)	53.45 $\pm$ 7.68	50.04 $\pm$ 7.29	0.0962
LF (n.u.)	46.26 $\pm$ 4.91	60.82 $\pm$ 6.02	0.0021
HF (n.u.)	53.74 $\pm$ 4.91	39.18 $\pm$ 6.02	0.0021
LF/HF (ln)	-0.19 $\pm$ 0.23	0.49 $\pm$ 0.29	0.0026
SDNN/RMSSD	1.24 $\pm$ 0.09	1.57 $\pm$ 0.13	0.0006
CSI	2.25 $\pm$ 0.19	2.97 $\pm$ 0.27	0.0005
CVI	3.39 $\pm$ 0.10	3.45 $\pm$ 0.09	0.1082
SampEn	1.67 $\pm$ 0.06	1.52 $\pm$ 0.08	0.0275
FuzzyEn	1.27 $\pm$ 0.05	1.14 $\pm$ 0.06	0.0006
LLE	0.67 $\pm$ 0.01	0.64 $\pm$ 0.01	0.0004

see that as CSI increases from baseline to nausea state (Fig. 2a,b), there is a tendency toward parasympathetic blockade or unopposed sympathetic activity, thus giving the nausea state subplots a “cigar shape”. CSI was significantly higher during nausea than at baseline (Table I), and highly correlated with all metrics ( $p < 0.05$ ) but SDNN (Fig. 3).

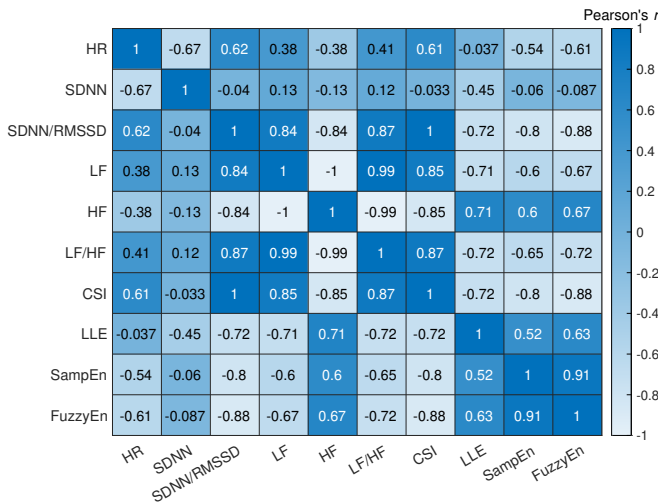


Fig. 3. Pearson correlation matrix of autonomic parameters.

Average SDNN/RMSSD was significantly increased from baseline (Table I) and strongly correlated with HR ( $p =$

0.0184) and all other metrics ( $p < 0.01$ ) except SDNN (Fig. 3). Consistent with the initial findings by [21], we found that SDNN/RMSSD index correlates strongly with LF/HF ratio ( $p = 5.97e-05$ ; Fig. 4) suggesting these indices may be characterizing HRV similarly but from different analytical standpoints.

Extending our analyses to HR and linear HRV indices; we found that average HR, SDNN, LF, and LF/HF were significantly increased during malaise (Table I). Moreover, as expected, HF power was markedly lower during nausea than at baseline; in particular, HF was strongly negatively correlated with SDNN/RMSSD ( $p = 1.78e-04$ ) and CSI ( $p = 1.30e-04$ ), and positively correlated with LLE ( $p = 4.42e-03$ ), SampEn ( $p = 2.40e-02$ ) and FuzzyEn ( $p = 8.65e-03$ ), Fig. 3. While there is a noticeable decrease in average RMSSD (Table I) during nausea compared to baseline; this however, did not reach statistical significance.

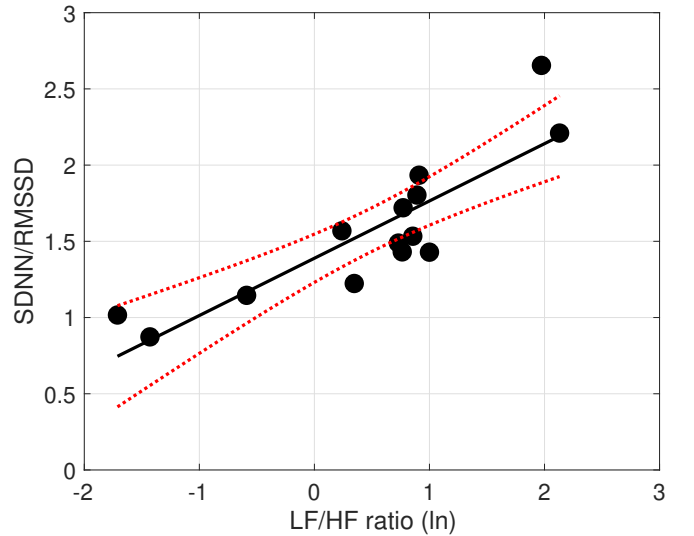


Fig. 4.  $\ln(\text{LF}/\text{HF})$  ratio responses of participants during nausea relate to increases in SDNN/RMSSD.  $\ln$  – natural logarithm.

#### IV. DISCUSSION

This paper presents first insights on the potential of nonlinear HRV metrics (i.e., SampEn, FuzzyEn and LLE), in

monitoring and assessing visually induced motion sickness; and thus advance our understanding of its elusive nature. We found a significant decrease in physiologic complexity and chaos during nausea compared to baseline. That is, patterns in the HRV signal were more predictable (more regular) during malaise than at rest.

The autonomic nervous function plays a large part in adapting to daily life stressors. This ability is driven by complex interactions owing to regulatory processes operating over multiple temporospatial scales [22]. Hence the long-held view that healthy heart rate dynamics are complex, and chaotic. In fact, aging and disease have long been implicated with negative affect on physiologic complexity [23]. In this light, our findings could be understood as diminution of irregularity and spontaneity during motion sickness-induced autonomic arousal. Denaturing this highly complex system, as we show here through an aversive experience such as motion sickness, or due to physical stress [17], the adaptive coping mechanisms of the system tend to reduce. This may also explain the polysymptomatic onset of motion sickness.

We utilised Poincaré maps to visually compare the topography of autonomic dynamics at rest and during nausea. Visually, the fitted ellipsoids during nausea state, shift to a longer and narrower area, depicting a “cigar-shape” (Fig. 2); as such, CSI response increases. This increase in cardiac sympathetic function was consistent with a previous study that used a motion video to induce motion sickness [8]. Accordingly, this suggests intensifying motion sickness may be triggering negative emotional valence; thereby, eliciting agitation. Moreover, it suggests interventions that alter sympathetic neural activity may prove efficacious in decreasing or hindering autonomic arousal arising from motion sickness.

Our results additionally support the association between SDNN/RMSSD and LF/HF during nausea (Fig. 4), whereas [21] introduced it while examining participants undergoing a 70° upright tilt test. Given its relatively straightforward computation, and proving sensitive to measuring motion sickness suggests it may be a useful complement or surrogate index to the LF/HF ratio in the context of motion sickness. Taken together, the newly reported measures herein may help us get closer to disentangling motion sickness-induced ANS perturbations.

## V. CONCLUSION

In conclusion, our results indicate in particular that (SamEn, FuzzyEn, LLE, SDNN/RMSSD) may be sensitive measures of motion sickness-induced nausea. Suggesting they could be used to complement the conventionally reported HRV indices when examining motion sickness. Moreover, these markers may have important implications as potent therapeutic targets for motion sickness. In addition to practical significance, that is, helping in automated malaise detection. Future studies are required to replicate our findings using a larger sample size. By extension, investigating other nonlinear indices (e.g., conditional, distribution and permutation entropies, etc.) may further enhance understanding of motion sickness.

## REFERENCES

- [1] J. F. Golding, “Motion sickness susceptibility,” *Auton. Neurosci. Basic Clin.*, vol. 129, no. 1, pp. 67–76, Oct. 2006.
- [2] J. Reason and J. Brand, *Motion Sickness*. Academic Press, 1975.
- [3] C. M. Oman, “Motion sickness: a synthesis and evaluation of the sensory conflict theory,” *Can. J. Physiol. Pharmacol.*, vol. 68, no. 2, pp. 294–303, 1990.
- [4] P. Matsangas, M. E. McCauley, and W. Becker, “The effect of mild motion sickness and sopite syndrome on multitasking cognitive performance,” *Hum. Factors*, vol. 56, no. 6, pp. 1124–1135, Sep. 2014.
- [5] J. R. Lackner, “Motion sickness: more than nausea and vomiting,” *Exp. Brain Res.*, vol. 232, no. 8, pp. 2493–2510, 2014.
- [6] J. Kim, V. Napadow, B. Kuo, and R. Barbieri, “A combined HRV-fMRI approach to assess cortical control of cardiovagal modulation by motion sickness,” in *2011 Annual International Conference of the IEEE Engineering in Medicine and Biology Society*, Aug 2011, pp. 2825–2828.
- [7] C.-T. Lin, C.-L. Lin, T.-W. Chiu, J.-R. Duann, and T.-P. Jung, “Effect of respiratory modulation on relationship between heart rate variability and motion sickness,” in *2011 Annual International Conference of the IEEE Engineering in Medicine and Biology Society*, Aug 2011, pp. 1921–1924.
- [8] A. D. Farmer *et al.*, “Visually induced nausea causes characteristic changes in cerebral, autonomic and endocrine function in humans,” *J. Physiol.*, vol. 593, no. 5, pp. 1183–1196, 2015.
- [9] M. Toichi, T. Sugiura, T. Murai, and A. Sengoku, “A new method of assessing cardiac autonomic function and its comparison with spectral analysis and coefficient of variation of R–R interval,” *J. Auton. Nerv. Syst.*, vol. 62, no. 1, pp. 79–84, 1997.
- [10] P. C. Ivanov *et al.*, “Multifractality in human heartbeat dynamics,” *Nature*, vol. 399, no. 6735, pp. 461–465, 1999.
- [11] S. A. A. Naqvi, N. Badruddin, A. S. Malik, W. Hazabbah, and B. Abdullah, “Does 3D Produce More Symptoms of Visually Induced Motion Sickness?” in *2013 35th Annual International Conference of the IEEE Engineering in Medicine and Biology Society (EMBC)*, 2013, pp. 6405–6408.
- [12] H. Ujike and H. Watanabe, “Effects of stereoscopic presentation on visually induced motion sickness,” in *Stereoscopic Displays and Applications XXII*, vol. 7863. SPIE, 2011, pp. 357 – 362.
- [13] T. Irmak, D. M. Pool, and R. Happee, “Objective and subjective responses to motion sickness: the group and the individual,” *Exp. Brain Res.*, vol. 239, no. 2, pp. 515–531, 2021.
- [14] Task Force of the European Society of Cardiology the North American Society of Pacing Electrophysiology, “Heart rate variability: Standards of measurement, physiological interpretation, and clinical use,” *Circulation*, vol. 93, no. 5, pp. 1043–1065, 1996.
- [15] J. Pan and W. J. Tompkins, “A Real-Time QRS Detection Algorithm,” *IEEE Trans. Biomed. Eng.*, vol. BME-32, no. 3, pp. 230–236, Mar. 1985.
- [16] J. S. Richman and J. R. Moorman, “Physiological time-series analysis using approximate entropy and sample entropy,” *Am. J. Physiol. Heart Circ. Physiol.*, vol. 278, no. 6, pp. H2039–H2049, 2000.
- [17] E. E. Solís-Montufar, G. Gálvez-Coyt, and A. Muñoz-Diosdado, “Entropy Analysis of RR-Time Series From Stress Tests,” *Front. Physiol.*, vol. 11, 2020.
- [18] W. Chen, Z. Wang, H. Xie, and W. Yu, “Characterization of Surface EMG Signal Based on Fuzzy Entropy,” *IEEE Trans. Neural Syst. Rehabil. Eng.*, vol. 15, no. 2, pp. 266–272, Jun. 2007.
- [19] M. T. Rosenstein, J. J. Collins, and C. J. De Luca, “A practical method for calculating largest Lyapunov exponents from small data sets,” *Physica D*, vol. 65, no. 1, pp. 117–134, 1993.
- [20] M. Brennan, M. Palaniswami, and P. Kamen, “Poincaré plot interpretation using a physiological model of HRV based on a network of oscillators,” *Am. J. Physiol. Heart Circ. Physiol.*, vol. 283, no. 5, pp. H1873–H1886, 2002.
- [21] R. Balocchi, F. Cantini, M. Varanini, G. Raimondi, J. M. Legramante, and A. Macerata, “Revisiting the potential of time-domain indexes in short-term HRV analysis,” *Biomed Tech (Berl)*, vol. 51, no. 4, pp. 190–193, 2006.
- [22] L. A. Lipsitz and A. L. Goldberger, “Loss of ‘Complexity’ and Aging: Potential Applications of Fractals and Chaos Theory to Senescence,” *JAMA*, vol. 267, no. 13, pp. 1806–1809, Apr. 1992.
- [23] L. A. Lipsitz, “Age-related changes in the “complexity” of cardiovascular dynamics: A potential marker of vulnerability to disease,” *Chaos*, vol. 5, no. 1, pp. 102–109, 1995.